Heliyon 10 (2024) e31306

Contents lists available at ScienceDirect

Heliyon

journal homepage: www.cell.com/heliyon

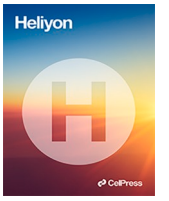

Research article

A novel approach to design chimeric multi epitope vaccine against *Leishmania* exploiting infected host cell proteome

Sooram Banesh [a], Neharika Gupta [a,1], Chethireddy Vihadhar Reddy [a,1], Uppuladinne Mallikarjunachari [b], Nupoor Patil [a], Sonavane Uddhavesh [b], Prakash Saudagar [a,*]

[a] *Department of Biotechnology, National Institute of Technology-Warangal, Warangal, 506004, Telangana, India*
[b] *High Performance Computing - Medical and Bioinformatics Applications, Centre for Development of Advanced Computing (C-DAC), Pune, Maharastra, India*

ARTICLE INFO

Keywords:
Epitope
Chimeric
Vaccine
Immune response

ABSTRACT

Leishmaniasis is a major infectious disease having high mortality which could be attributed to lack of a suitable vaccine candidate. We propose a novel approach to design multiepitope vaccine to leishmaniasis exploiting specific membrane proteome from infected macrophage from host. The MHC-I, MHC-II and BC epitopes predicted for unique proteins from the infected macrophages and *Leishmania* and a MEV designed in various combinations (1a-1m). The epitope arrangements 1a, 1k, 1l, and 1 m showed a strong antigenicity profile and immune response. The molecular dynamics simulation indicate the 1k, 1l, and 1 m constructs have strong affinity toward TLR-2, TLR-3, and TLR-4. Overall the structural and immunogenicity profile suggests 1k is top candidate. Further, a computational model system with TLR-2, TLR-3, TLR-4, BCR, MHC-I and MHC-II was generated for 1k construct to understand the MEV interactions with immune components. Dihedral distribution and distance was enumerated to understand the movement of immune components towards 1k. The results indicate 1k has strong affinity for the immune response molecules especially TLR-3, BCR and MHC-II are coming in close contact with the MEV through the simulation. The study suggests that designed multi-epitope vaccine 1k has potential to induce proper immune response but warrants further studies.

1. Introduction

Leishmaniasis is a neglected vector-borne disease caused by an obligatory intracellular parasitic protozoan called *Leishmania*. *Leishmania* (Kinetoplastida:Trypanosomatidae) is a unicellular eukaryotic organism with a distinct nucleus and kinetoplast [1]. Around 20 out of 53 *Leishmania* species, that infect animals and reptiles, have been linked to human infections [2]. According to WHO (2021), each year around 0.7–1 million cases are recorded throughout the world, with 20000–30000 deaths occurring annually and is one of the seven most significant tropical diseases with a wide range of clinical manifestations and potentially deadly outcomes [3]. The disease is prevalent mainly in tropical and subtropical regions, particularly in Africa, Brazil, Algeria, Afghanistan, Columbia, Iran, Sri Lanka, and India. Leishmaniasis has three main clinical manifestations: visceral leishmaniasis (VL), cutaneous leishmaniasis (CL),

* Corresponding author.
E-mail address: ps@nitw.ac.in (P. Saudagar).
[1] Equal contribution.

https://doi.org/10.1016/j.heliyon.2024.e31306
Received 13 September 2023; Received in revised form 14 May 2024; Accepted 14 May 2024
Available online 17 May 2024

and mucocutaneous leishmaniasis (MCL).

The lifecycle of *Leishmania* is dependent on two hosts i.e. it possesses a digenetic lifecycle. The definitive host is humans and the intermediate host is a sandfly (insect vector) [4]. It shuttles in between two morphologically differentiated forms: extracellular flagellated and motile promastigotes (in the alimentary canal of sandflies) and intracellular non-flagellated and non-motile amastigotes (in the phagocytic cells of mammalian hosts) [5]. The parasite's complex life cycle makes it difficult to prevent disease transmission and infection. Since there is no progress in vaccine development, chemotherapeutic drugs such as pentavalent antimonials, miltefosine, paromomycin and amphotericin B are currently used for the treatment of leishmaniasis [6]. Despite the fact that these chemotherapeutic medications are readily available for treatment, their usage is limited due to several side effects such as relapse of infection, reduced efficacy, renal toxicity, rising drug resistance and greater treatment costs [7]. These anti-leishmanial drugs can cure the existing cases but new cases are emerging day by day. So, for complete eradication of leishmaniasis, vaccination is the most efficient method.

Whole-killed parasite such as Leishvaccine (whole-killed promastigotes of *Leishmania amazonensis* and Bacillus Calmette–Guérin (BCG) became somewhat successful in the prevention of canine leishmaniasis but did not got approval from WHO for treatment in humans [8]. Fractionated *Leishmania* antigen vaccine such as Leishmune® and CaniLeish® and live-attenuated form of *Leishmania infantum* have also shown remarkable success against canine leishmaniasis but not against human disease [9].

Since there is no licensed vaccine for human leishmaniasis or for that matter effective protection against leishmaniasis, immunoinformatics-based computational vaccinology can be utilized to design a chimeric multi-epitope vaccine [10]. The first successful immune-informatics-based vaccine was designed against *Neisseria meningitidis* by Adu-Bobie et al. [11]. Later on, many such vaccines have been designed and are used clinically. In this study, we have identified the membrane proteins from *Leishmania* parasite as well as from *Leishmania*-infected macrophages and designed a chimeric multiepitope-based vaccine construct. Because of the presence of specific B- and T-cell epitopes, these proteins are immunogenic in nature and are recognized by surface receptors on antigen-presenting cells (APC), T-cells, and other immune cells. The formation of complexes between B/T-cell epitopes and surface receptors triggers a cascade reaction of cellular/humoral immune response that kills the parasites. This approach entails mapping immuno-dominant B and T cell epitopes in an antigenic protein, evaluating their immunogenic potential, integrating them with suitable linkers, and testing their ability to bind host cell receptors. Instead of utilizing complete proteins or antigens, immunoinformatics creates chimaeras using specific protein epitopes. Further, the multi immune component system with vaccine construct was designed and simulated to understand the specific movement of vaccine construct 1k towards other immune components such as TLR-2/3/4 or MHC-I/II or BCR (B-cell receptor). The movement of TLR-2, TLR-3 and MHC-II indicate the 1k has strong potential as vaccine candidate. Overall the study highlights the effectiveness of designed vaccine construct against *Leishmania* however further investigation needed to understand it's real time effect immune system or providing protection against parasite.

2. Methodology

2.1. Collection and screening of Leishmania infected macrophage proteome

The *Leishmania* infected macrophage proteome profiles from mouse and human were obtained from literature [12,13]. There are several proteins that have been shown to express in *Leishmania* infected macrophages and we have extracted the proteins that localized to membrane and further screened based on the explicit and uniqueness to infected macrophages (present in 12 or 24 h post infection) only. The finalized proteins were used to predict MHC-I, MHC-II, BCE and IFN-γ epitopes for further studies.

2.2. Collection and identification of antigenic proteome for Leishmania

The entire proteome of *Leishmania donovani* was retrieved from the UniProt database. The proteins embedded in the plasma membrane region were predicted using the DeepLoc 2.0 webserver [14]. DeepLoc 2.0 uses a deep-learning approach to predict subcellular localization based on the characteristics generated from the protein sequence. The proteome was submitted in the DeepLoc to retrieve the transmembrane proteins. Two criteria were followed to sort the entry sequences viz. the entries that showed their subcellular localization in the cell membrane and threshold prediction score of 0.7 or higher. The protein entries satisfying the criteria were considered for further analysis. The entries selected were then submitted in BLAST to check their alignment patterns. The sequences that did not show any overlap with the proteome of *Homo sapiens* were considered further. These entry sequences were then submitted to Deep-TMHMM to study the protein topology [15]. The residues spanning the extracellular region of the plasma membrane were retrieved and curated for further analysis.

2.3. Prediction of CTL, HTL, B-cell epitope and IFN-γ epitopes

The prediction of CTL epitopes was done in NetMHC 4.0 [16] using the default parameters. NetMHC 4.0 uses artificial neural networks for predictions of major histocompatibility complex I (MHC-I). It uses both affinity and elution data from Immune Epitope Database and Analysis Resource (IEDB) [17] respectively. Similarly, the prediction of HTL epitopes was done by submitting the retrieved extracellular peptide sequences in NetMHCII pan 3.2 [18] using the default parameters. It uses artificial neural networks for predicting pan-specific binding of peptides for MHCII HLA isotypes. The prediction of B-cell epitopes was done by submitting the retrieved extracellular peptide sequences in BepiPred 3.0 [19] using default parameters. It uses protein language models for high-accuracy linear and conformational epitope prediction.

After the prediction of CTL, HTL and continuous B-cell epitopes by using the above-mentioned servers by neural network algorithms, all the epitopes of CTL, HTL and B cells in FASTA sequence were aligned in MULTALIN server with its default parameters to obtain overlapping epitopes. The overlapping epitopes were selected as CTL- B cells epitopes, HTL- B cell epitopes and CTL-HTL-B cell epitopes. The INF- **γ** is a cytokine, a member of type-II interferon family with anti-viral, anti-tumor and immunomodulatory functions [20]. It triggers the activation of the immune response and stimulates the elimination of pathogens [20]. IFN **γ** is primarily secreted by Natural killer cells (NK cells), $CD8^+$ and $CD4^+$ T cells [21]. The overlapped epitopes were selected and submitted to the IFNepitope server [22] to determine their effectualness in inducing Antigenicity or pathogenicity by producing IFN γ. The algorithmic approach for epitope prediction was the Motif- Support Vector Machine (SVM) Hybrid approach and the model used for the prediction was IFN gamma versus Non IFN gamma model epitopes datasets from IEDB database.

2.4. Design and analysis of vaccine candidate

The basis of this study is to use epitopes against infected host macrophages in combination with the infectious agents *Leishmania*. When antibodies generated, they can act not only on free parasite but also on host cells that are being infected with parasite [23]. The BCE, HTL and CTL epitopes generated for infected macrophage proteins or *Leishmania* specific proteins were joined using specific linker peptides. In addition, the TLR-4 agonist RS09 shown to be effective in inducing protective cytokine secretion hence TLR-4 agonist is added to the vaccine construct [24]. The B-cell epitopes were connected by KK stretch whereas HTL and CTL epitopes were joined by GPGPG and AAY peptide stretches respectively. The sequences are arranged in TLR-agonist, BCE, HTL and CTL from N-terminal to C-terminal respectively so that the sequence result in stable and high yield construct as reported earlier [25]. The constructed vaccine is evaluated for antigenicity, allergenicity and the similarities with other host protein sequences using antigenic peptide prediction tool, AllerTOP server [26] for allergenicity and NCBI P-BLAST [27] for sequence similarity. Further the designed vaccine candidate is analysed for toxicity using Toxinpred Server [28].

To determine the 3D structure of the vaccine construct, Alphafold colab was used. This tool produces structures with great accuracy and precision. The physical and chemical properties of the vaccine construct were assessed by ProtParam web tools (https://web.expasy.org/cgi-bin/protparam/protparam). The tool evaluates parameters like molecular weight, theoretical pI, amino acid and atomic composition, aliphatic index, instability index and grand average of hydro-pathicity (GRAVY). To predict the protein solubility, Protein–Sol tool was used. The predicted 3D model of the designed vaccine was validated using PROCHECK server [29] and ProSa webserver [30]. The server analyses residue by residue geometry to determine the stereochemical quality of a protein structure. It produces Ramachandran plot, chi-chi plots, main and side chain parameter plots and bond length graphs to validate the tertiary structure. ProSa server also predicts and compares with existing X-Ray and NMR crystal structures whether the structure has good conformation.

2.5. In- silico simulation of immune response against vaccine candidate

The designed vaccine candidate before going into in-vitro studies need to understand whether the construct induce immune response. The C-IMMSIM server [31] was used to simulate the immune response against the designed vaccine constructs 1a-1m. The C-IMMSIM webserver is based on position specific scoring matrix to simulate the immune response. The simulation was conducted for 366 days (a total of 1098 steps) with each injection contains 1000 antigen molecules. A total of two injections were used in this simulation.

2.6. Molecular docking and interaction analysis

The designed vaccine candidate assessed for its ability to interact with TLRs. The structures for TLR-2, TLR-3 and TLR-4 were obtained from protein data bank. The vaccine constructs 3D models obtained from Alphafold server [32]. The vaccine 3D model energy minimized before docking using Swiss PDB viewer. The TLR-4 (PDB id: 2Z63) and TLR-3 (PDB id: 7WV3) or TLR-2 (PDB id: 6NIG) were retrieved and pre-energy minimized before submitting to the docking server Cluspro [33]. The best docking conformation was analysed for protein-protein interactions using Ligplot + v2.2.8 [34].

2.7. Stability analysis of vaccine-TLR complexes

The molecular dynamics simulation studies were employed to understand the stability of the designed vaccine-TLR complexes. The molecular complexes obtained from ClusPro were energy minimized and removed any non-standard residue or naming in the structures. The complexes were prepared using XLeap module of AMBER tools [35]. The complexes were solvated, energy minimized and equilibrated (NPT ensemble) to a temperature of 300 K and a pressure of 1 atm with position restraints on heavy atoms. The production simulations were performed conducted for 100 ns without restraints, and trajectories generated were analysed for used to calculate the Root-mean-square deviation (RMSD) of the protein backbone atoms using cpptraj module of AMBER20 [36].

2.8. Composite immune system model generation and analysis for designed vaccine candidate

CHARMM-GUI server [37] multicomponent assembler module is used to generate a composite immune system model consisting of MHC-I, MHC-II, BCR, TLR-2, TLR-3, TLR-4, and multi-epitope vaccine construct (MEV). All of the molecules further prepared using

Xleap module of AmberTools [35]. The system is solvated using TIP3P water box and Na + ions were added. The complex is energy minimized and equilibrated at NVT. Initially a 1 ns simulation carried out at NPT conditions to see whether system holds intact. The simulations were extended further for another 100 ns. All of the simulations were carried out using AMBER20 [36]. The MD trajectory was analysed for stability, conformations free energy changes, and Ramachandran plot distributions. The trajectories were analysed for distance changes between immune components and MEV. AMBER CPPTRAJ program distance module was used to calculate distance between MEV-TLRs, MEV-MHC-I and II and MEV-BCR. The obtained distance values were normalized and plotted to understand whether any immune components moved towards MEV.

2.9. In-silico cloning and expression analysis

The protein sequence reverse transcribed and converted to DNA codon in Java Codon adaptation tool [38]. The sequence is optimized to enable expression in *Escherichia coli* (strain K12) strain. Besides, restriction sites (*Bam*HI, and *Xho*I) were introduced at 5′ and 3′ ends, respectively. The final sequence was then cloned into the pET-28a (+) vector with a C-terminal 6X-Histidine tag followed by stop codon. Further the expression of the protein sequence was analysed using *E.coli* expression prediction system. The expression analysis and residue stretches that favour solubility was analysed using ccSOLomics server (https://s.tartaglialab.com/update_submission).

3. Results

3.1. Identification of strong binding epitopes for CTL, HTL, and B-cells

The idea behind this work is to use epitopes from host proteins such as infected macrophages along with parasite antigenic epitopes to generate the vaccine. Earlier studies have suggested that the macrophages infected with *Leishmania* show distinct protein expression

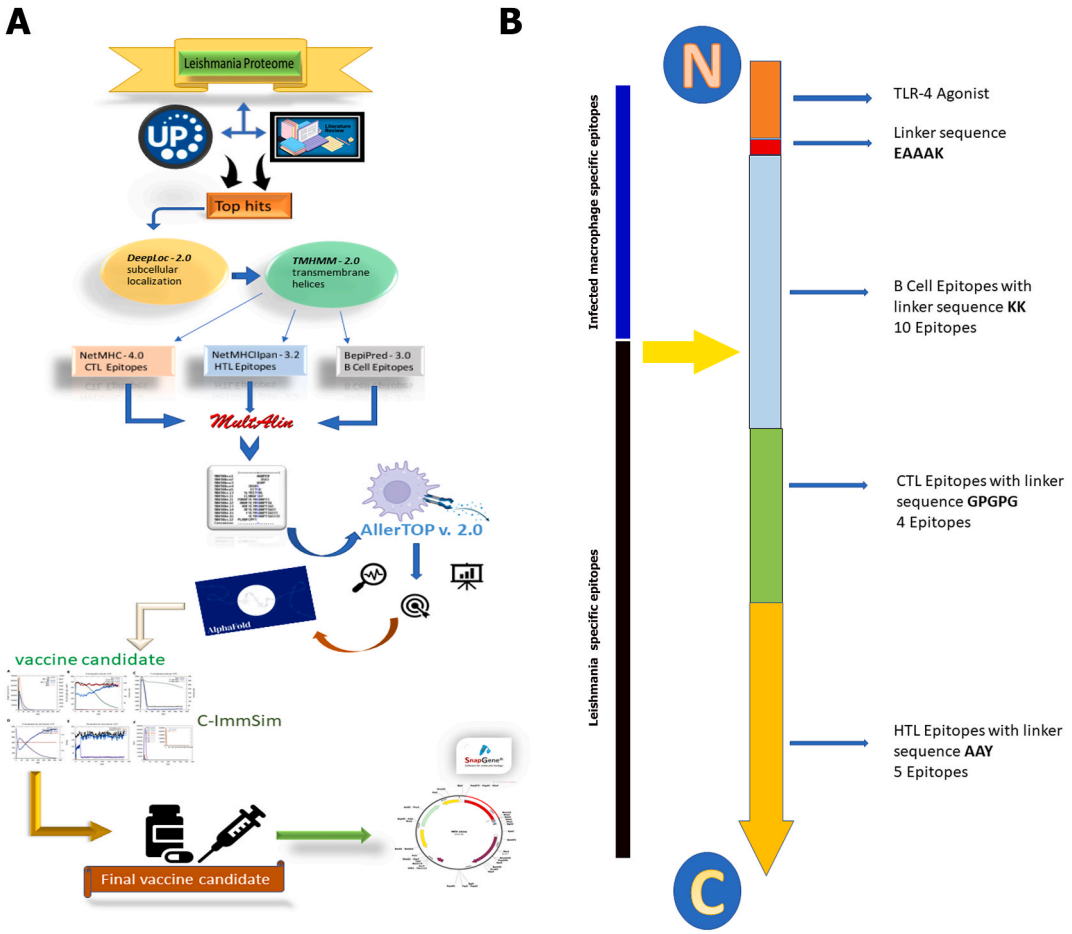

Fig. 1. General work flow and design of multi-epitope vaccine. A). The immunoinformatics approach used in the study and steps involved in the designing vaccine.

on their surface compared to non-infected cells [12]. The proteins which are suggested to be exclusive in *Leishmania* infected macrophages were identified and transmembrane regions were determined using DeepTMHMM. The proteins further segregated into plasma membrane or cytosolic, using DeepLoC server. The cell membrane proteins chosen due to their exposure to the outer cell surface that facilitates the detection by immune cells. A total of 16 such proteins were found to be unique to the infected macrophages including some of the hypothetical proteins such as LOC75734, and LOC109168 [12]. The extracellular domains of the proteins were submitted to NetMHC and NetMHC-II predicted a total of 2250 cytotoxic T lymphocyte (CTL) epitopes, and 2210 helper T Lymphocyte (HTL) epitopes, respectively. Based on the threshold of $\leq$0.5 and $\leq$2.0 percentile rank for CTL and HTL respectively, 22 CTL and 34 HTL epitopes were selected as strong binders.

Similarly, the whole cell proteome of *Leishmania donovani* has been obtained from UniProt database. The unknown proteins of origin or hypothetical proteins have been excluded from the list. The final list of proteins were further screened for transmembrane regions and their localization. A total of 500 proteins were analysed for transmembrane domains and localization. Further, the HTL and CTL were predicted. A total of 1254 number of HTL and 1871 number of CTL were identified. The strong binders have been identified based on affinity score from the NetMHC servers and included for design of multiepitope vaccine. Finally, B cell epitopes were predicted using BepiPred server and used them to identify overlapping sequences using MULTALIN server.

Adjuvants facilitate in enhancing or shaping the immune response against vaccines [39]. For multi-epitope vaccines, use of peptide adjuvants mainly TLRs agonist could be proven beneficial in inducing the appropriate immune response [40]. A peptide RS09 was used as adjuvant to construct vaccine. RS09 was reported to induce strong immune response in in-vitro condition [41]. Use of the RS09 could facilitate enhanced immune response toward MEV. General flow of the work (Fig. 1A) and assembly of vaccine construct is represented in (Fig. 1B). The epitopes obtained from unique surface proteins of *Leishmania* infected macrophages were arranged forefront of vaccine construct and *Leishmania* specific antigenic epitopes were arranged next to them (Fig. 1B). The epitopes used to construct the vaccine candidates were listed in (Supplementary data-1).

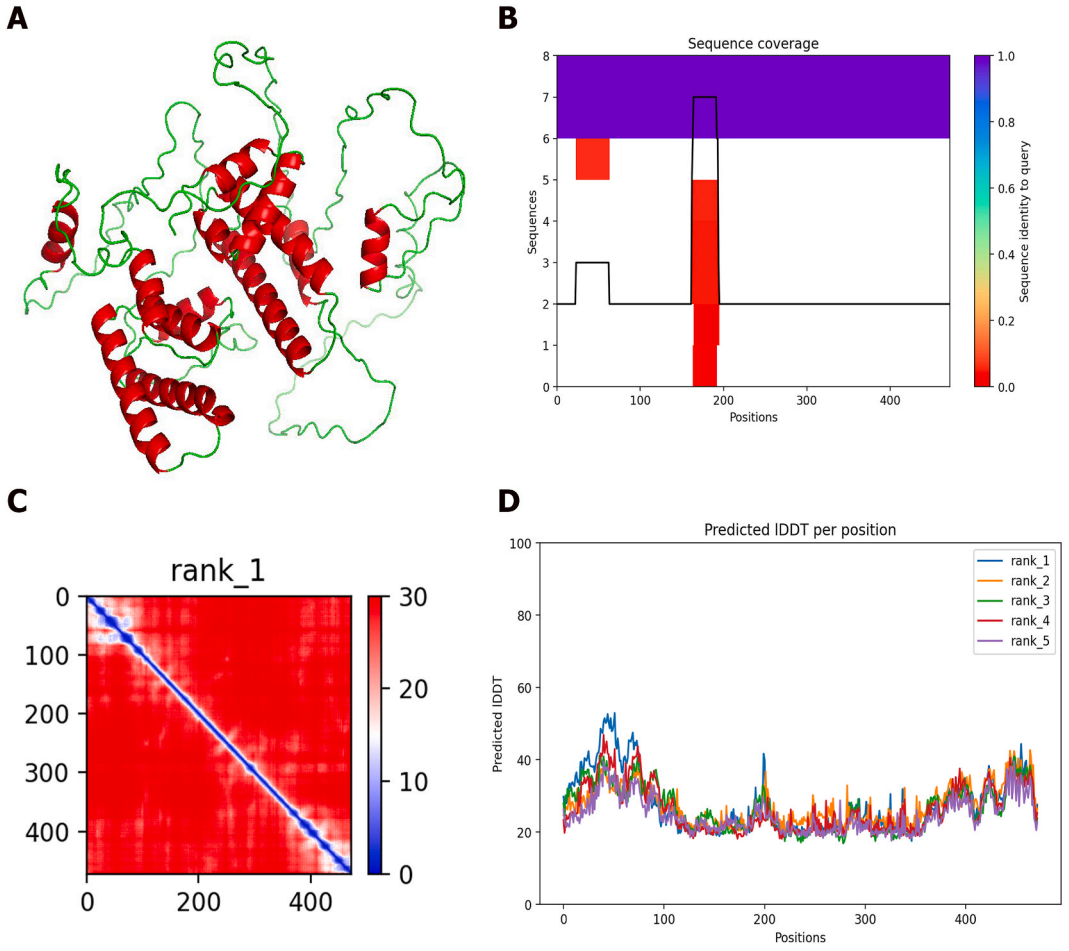

Fig. 2. Designed 3D models for vaccine construct. The vaccine construct sequence (1a) is submitted to Alphafold colab. The panel A) shows the 3D model of the construct.

3.2. Design and structure analysis of multi-epitope vaccine constructs

The arrangement of epitopes in a vaccine plays crucial role in inducing the immune response [42]. In order to find optimum vaccine construct that not only target *Leishmania* but also infected macrophages, we have generated scrambled library of constructs (1a-1m) (Supplementary data 1). Initially, the constructs were analysed for immunogenicity (Vaxijen2.0 score) to categorize them onto immunogenic or non-immunogenic. The construct 1a-1j showing the antigenic score of 0.44–0.48 which is below the threshold value 0.5, for vaccines against parasites. Surprisingly the randomized arrangements 1k, 1l, 1 m showed 0.523, 0.502 and 0.502 respectively (Supplementary data 1). Out of the designed constructs, 1k was found to be a prominent antigen as suggested by the antigenic score.

The structure of multi-epitope vaccine is crucial as it holds key to interactions with immune cells, the arrangements now submitted to Alphafold colab cloud server for structure prediction. The molecular models generated from the vaccine sequences were found to be consistently featuring more random coil content except 1a, 1k, 1l, and 1 m (Fig. S1). For 1a construct, rank 1 model coverage, PAE score and pLDDT scores given in Fig. 2. The models 1a, 1k, 1l and 1 m has random coil, alpha in equal ratio whereas beta sheet content is less. Hence, 1a, 1k, 1l, and 1 m models further analysed for structural integrity using protein-model validation tools. The models initially assessed by Ramachandran plot (PROCHEK server) followed by ProSA (model quality) and ProtSAV (comparison of model with structure validation algorithms). Most of the residues in constructs 1a and 1k were found to be featuring in mostly allowed regions whereas large number of residues in 1l and 1 m are mostly outside the allowed regions (Fig. 3A–i, B-i, C-i, and D-i). Similarly, the 1a and 1k constructs were found to be within the range of global z-score whereas other constructs (1l, and 1 m) were showed z-values that are not fit with global XRD or NMR structure profiles (Fig. 3A–ii, B-ii, C-ii, and D-ii). Besides, the models are validated for their structural integrity using ProtSAV webserver. Out of the four constructs only 1a was found to be in green zone for at least one prediction algorithm (ERRAT) whereas other three constructs were found to be validated by ProQ algorithm (Fig. 3A–iii, B-iii, C-iii, and D-iii). The result indicates the structures 1a and 1k were structurally well designed and could be used as a vaccine candidates.

Further, the structures were subjected to a short (50 ns) molecular dynamics simulations to ascertain overall stability and quality for the models (Fig. 4). The RMSD value for construct 1a showed slight fluctuation though converged at the end of the 50 ns (Fig. 4A–ii) whereas 1k, 1l, and 1 m constructs perfectly converged as suggested by flattened RMSD value started at 20 ns and lasted till the end of simulation (Fig. 4B–ii, 4C-ii, and 4D-ii). The RMSD value for all of the constructs suggests the structure is intact and has no perturbations through the simulation. The compactness or folding of the vaccine models was analysed using radius of gyration. Construct 1a and 1 m showed improper folding or compactness as evident from fluctuating radius of gyration values (Fig. 4A–iii, 3D-iii). On the

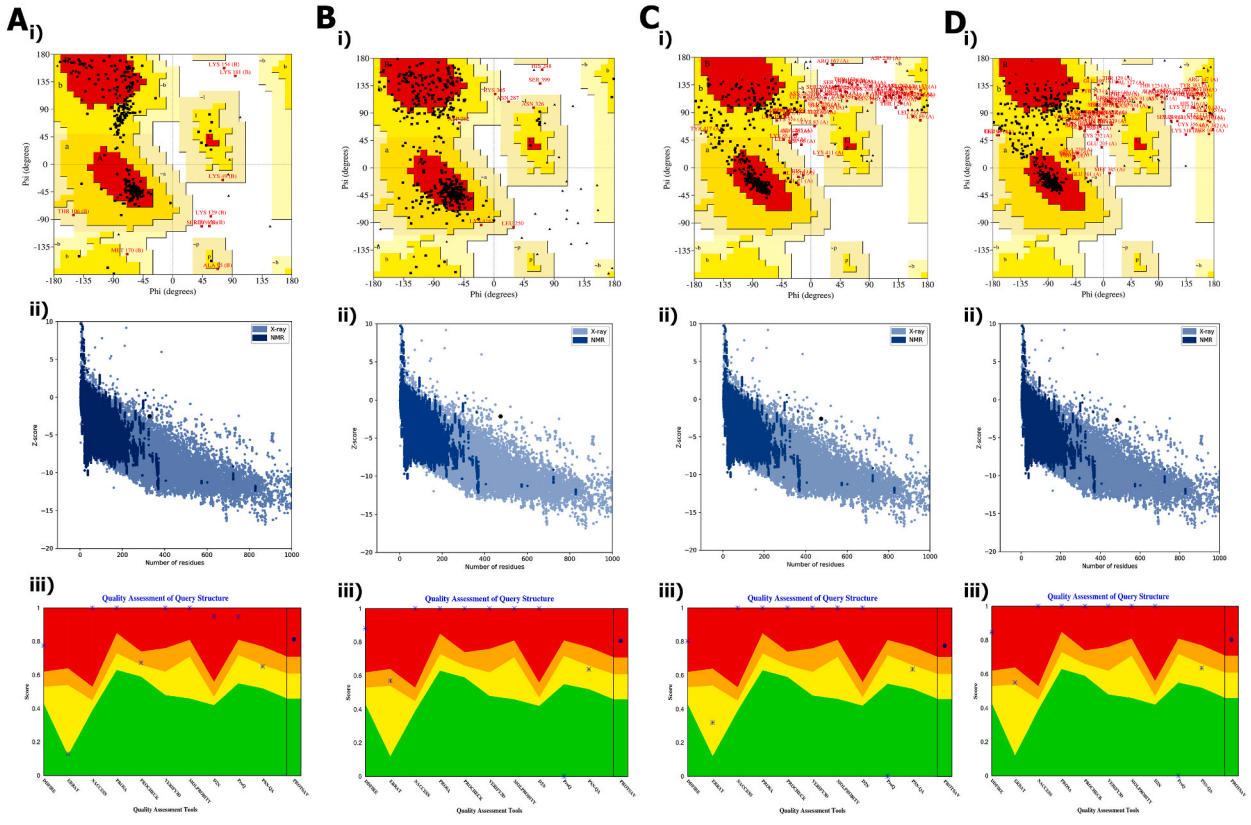

Fig. 3. Multiepitope vaccine construct structure validation. For all panels i. Ramachandran plot, ii. ProSa conformations comparison within the existing X-ray and.

other hand the constructs 1k, and 1l were found to be properly folded and indicates the compactness of the models (Fig. 4B–iii, 3C-iii). Similarly the RMSF and SASA were analysed for the constructs (Fig. 4A–D, iv and v). The residue fluctuation was more (~2 nm) for 1a and 1l constructs. Especially the residue stretches 120–130 (for 1a) and 215–250 (for 1l) indicate these regions have improper dihedrals or steric clashes. (Fig. 4 A, B, C, D –iii panels). Interestingly, all of the constructs showed decrease in solvent accessible surface area over the simulation suggests that the structures favour stable protein-protein interactions which could be useful to interact with immune system components such as TLRs. Overall the MD simulation studies indicate the constructs 1k, and 1l are stable through the simulation.

3.3. *In-silico evaluation of therapeutic suitability of designed vaccine constructs*

For a vaccine to be suitable, it should be devoid of any allergenicity, and toxicity but should have strong immunogenicity. All four short listed vaccine constructs (1a, 1k, 1l, and 1 m) were initially analysed for allergenicity and toxicity. All four protein constructs were found to be non-allergenic and non-toxic (Table 1). Further the constructs analysed for antigenicity score. The designed vaccine candidates have 327–400 residues with an average antigenic propensity score of 1.0241 as determined by the antigenic peptides prediction algorithm. The vaccine candidate consists 12–20 antigenic stretches among which the largest stretch contains 48 residues. The antigenic propensity score above 1 indicates the peptide stretches are potentially antigenic. The result indicates the designed vaccine would be immunogenic and a potential vaccine candidate. In addition, a vaccine candidate must be non-homologous to human proteins to avoid an auto-immune reaction/toxicity. The sequences alignment using NCBI Protein blast showed that none of the human proteins were homologous to the vaccine constructs (Fig. S1). The results suggest the designed vaccine could be safe in human use.

We further evaluated the vaccine constructs ability to induce immune response using C-IMMISM server. A total of two injections with each injection carrying 1000 antigen molecules were simulated for a 360 days' time frame. The simulated plots are represented in (Fig. 5). Upon injection of the first dose, the immunoglobulin (IgM, IgG1 + IgG2, and IgG + IgM) levels were elevated to several folds in constructs 1a (Fig. 5 A-i) and 1l (Fig. 5 C-i) whereas only IgM levels are spiked in constructs 1k (Fig. 5 B-i) and 1 m (Fig. 5 D-i). Though

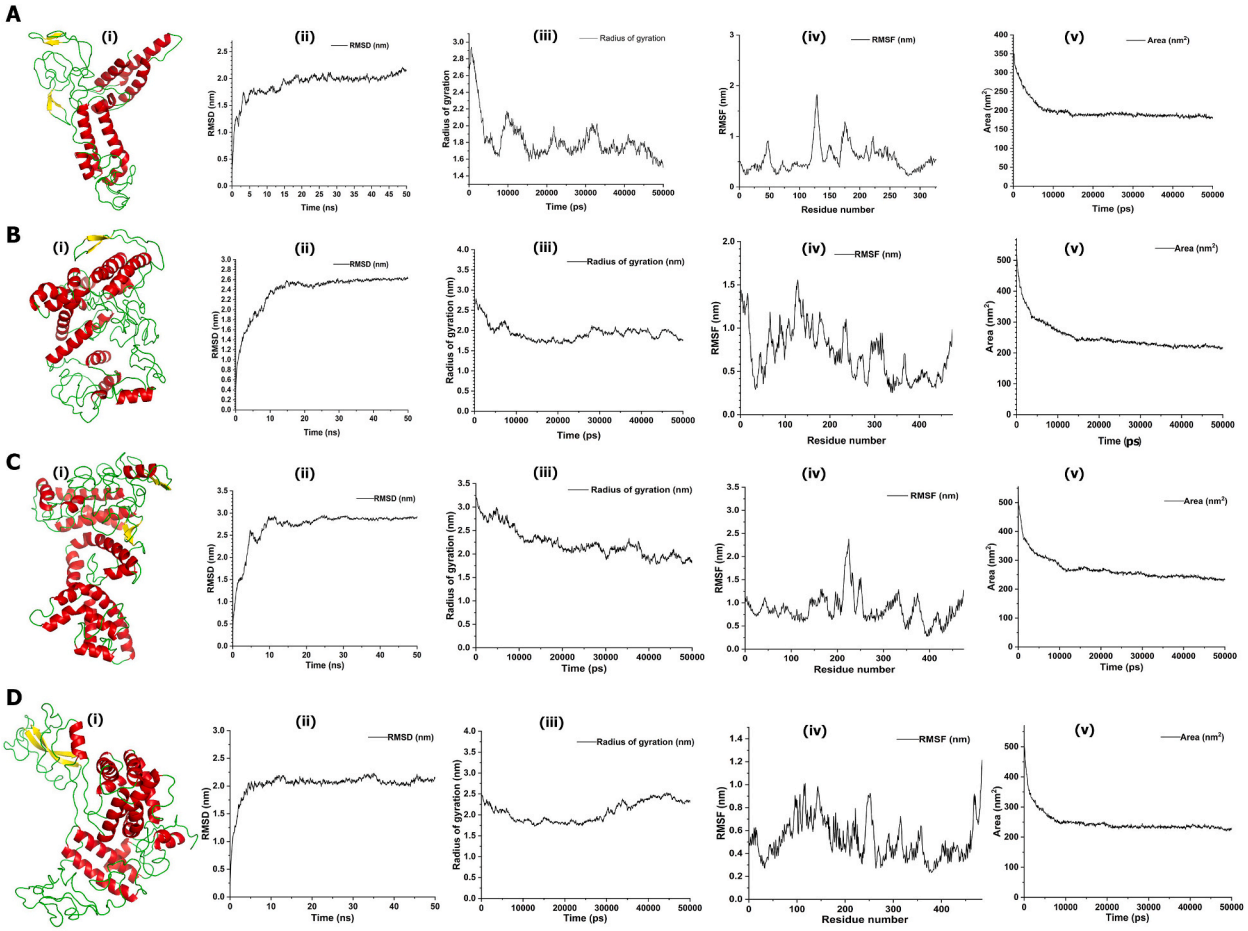

Fig. 4. Stability analysis for vaccine constructs. A) 1a construct structure and MD simulations. i). The 3D structure of 1a represents alpha helix (red), beta sheet (yellow). (For interpretation of the references to colour in this figure legend, the reader is referred to the Web version of this article.)

Table 1
Evaluation of vaccines constructs for their therapeutic suitability and immune response.

Construct	Toxicity	Allergenicity	Antigenicity	Vaxijen score	IgG + IgM Levels
1a	None	None	1.0295	0.4602	1.3×10^6
1b	None	None	1.0304	0.4678	1.59×10^6
1c	None	None	1.0300	0.4640	1.6×10^6
1d	None	None	1.0289	0.4454	1.42×10^6
1e	None	None	1.0286	0.4450	1.57×10^6
1f	None	None	1.0482	0.4820	1.43×10^6
1g	None	None	1.0482	0.4698	1.55×10^6
1h	None	None	1.0283	0.4560	1.55×10^6
1i	None	None	1.0283	0.4533	1.49×10^6
1j	None	None	1.0296	0.4544	1.5×10^6
1k	None	None	1.0311	0.5234	1.5×10^6
1l	None	None	1.0311	0.5022	1.51×10^6
1 m	None	None	1.0231	0.5025	1.4×10^6

IgM only spiked in 1k and 1l, this could be indication of secretion of effective neutralizing antibodies by B cells [43]. For all the constructs, the immunoglobulin production started after 5 days of injection. The response was lasted till 100 days or 150 days (for 1k and 1l). In contrast the response lasted for 350 days for constructs 1 m and 1a. However, the second dose, did not produce any significant change in immunoglobulin levels for 1k, 1l, and 1 m constructs. This data indicates the single dose of designed vaccine would be sufficient for adequate immune response. The single dose induced response without the booster dose is ideal for clinical vaccines. Further the B cell population, TH cell population, and TC cell population were analysed (Fig. 5 panels ii-iv for A, B, C, and D). All of the constructs showed large memory B cell spike upon injection which lasted for almost a year (Fig. 5 A-ii, B-ii, C-ii, and D-ii). Besides, the TH and TC cell population for active cells rapidly spiked after first injection and lasted for a year (Fig. 5 panel's iii-iv for A, B, C, and D). The response for most of the constructs was same and suggests all of the constructs effectively induces the immune response.

In addition, a high proliferation of both helper and cytotoxic T-cells was observed throughout the simulation. The macrophages population is also consistently high through the simulation (Supplementary data 2). Moreover, the cytokines IFN-γ, TGF-β, IL-10 and

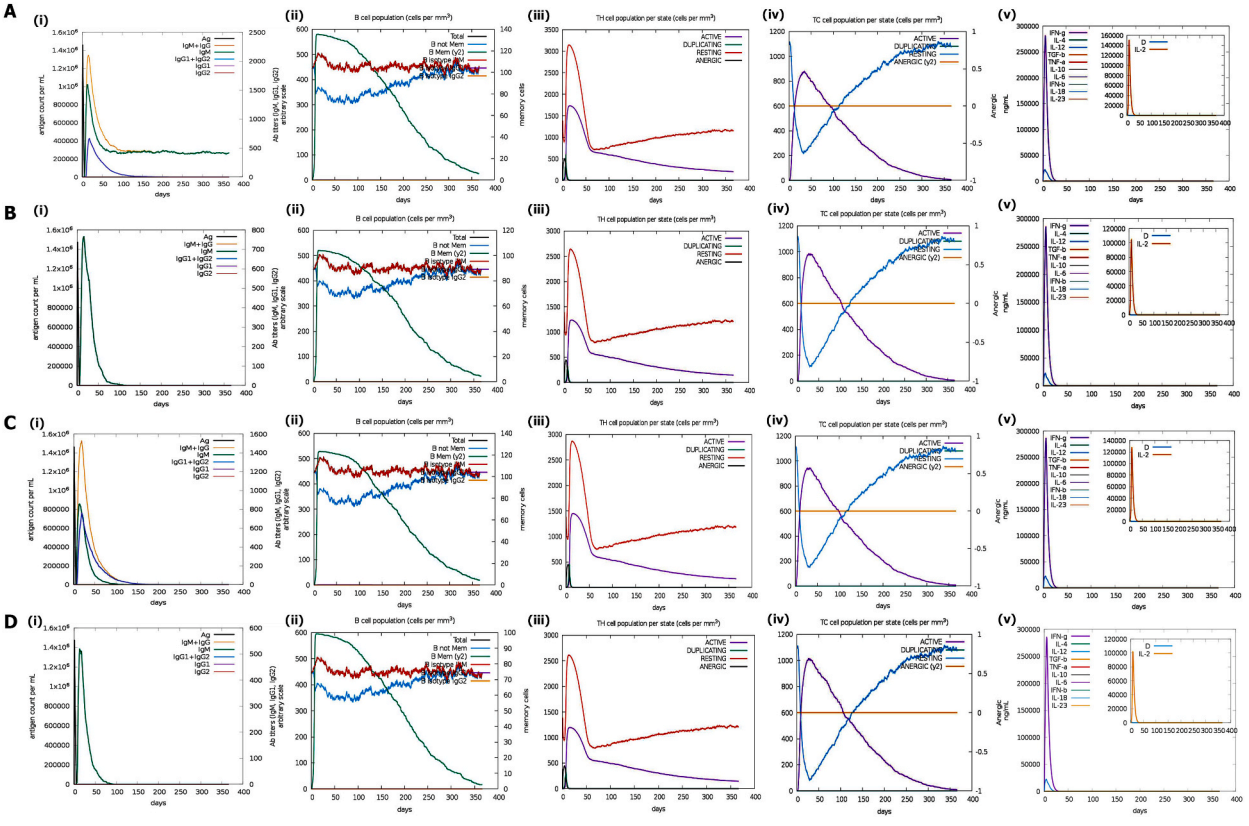

Fig. 5. Immune response simulation for designed vaccine constructs. A). 1a construct, B), 1k construct, C) 1l construct, and D) 1 m construct. Sub panels i.

IL-12 levels were found to be high and lasted for several days. Therefore, the designed multi-epitope vaccine constructs induces both humoral and cellular immune responses. The results also suggests the vaccine candidates would only need a single dose to induce optimal immune response which warrants in-vitro and in-vivo studies to ascertain the optimal dose.

3.4. Mapping the vaccine candidate interactions with TLR receptors

The crucial step in vaccine functioning is the innate recognition by host cell receptors [44]. Earlier studies suggested that TLR-2, 3, and 4 play crucial role in innate recognition of *Leishmania* and contribute to effective immune response [45]. A molecular docking was carried out between TLRs with vaccine constructs 1a, 1k, 1l, and 1 m. The constructs 1k, and 1l showed strong binding affinity towards TLR-3 with binding energy of −1137, −1243.2 kcal/mol respectively whereas 1 m showed strong affinity to TLR-4 (−1134.2 kcal/mol). The binding orientation of constructs with TLR-2, TLR-3 and TLR-4 were showed in (Fig. 6). Construct 1a was found to be weakly interacting with the TLR-2, TLR-3 and TLR-4 respectively (Fig. 6 A-i, ii, and iii). Besides the constructs 1 m and 1l were also found to be distant with the TLRs (Fig. 6 i, ii, iii panels for C and D). Contrast to the other constructs, 1k was found to embed within TLR-3 compared to other two TLRs (Fig. 6B–i, ii and iii) (Fig. 7). The interphase of the 1k residues interacting with TLR-3 is shown (Fig. 7A). The construct 1k immersed in the large groove of TLR-3 and could be a mediating factor for strong interactions (Fig. 7B, C, D). The results suggest the designed construct 1k favours the binding to TLR-2, TLR-3 and TLR-4 as compared to other TLRs. Previously it has been shown that TLR-3 is needed for recognition, phagocytosis and inducing IFN-γ primed macrophages for effective elimination of parasite [46]. The favoured binding of 1k to TLR-3 could be beneficial as it invokes the phagocytosis which could contribute to eliminate the parasite and generating proper immune response against parasite.

Further, the TLR-1k interaction, and distance heat map for TLR-1k residues was ascertained to understand the type of interactions and residues involved (Fig. 8 A, B, and C, upper panel-interaction plot, lower panel-distance heat map). The TLR-1k interaction analysis suggests 1k is strongly interacting with TLR-3 and TLR-4 with several residues participating in the hydrogen bonding (Fig. 8 A, B, and C, upper panel-interaction plot) (Table 2). More importantly the residues Glu53, Arg100, Arg112, and Glu113 consistently featuring in TLR-3 and TLR-4 whereas Arg100 found to be common for all three complexes. The distance map was constructed with 8 Å cut-off between hydrogen bond acceptor and hydrogen bond donor. The results suggest the 1k interactions with TLR-3 and TLR-4 has more density of hydrogen bonds with strong donor-acceptor network. Overall, the results highlight 1k has high affinity towards TLR-3

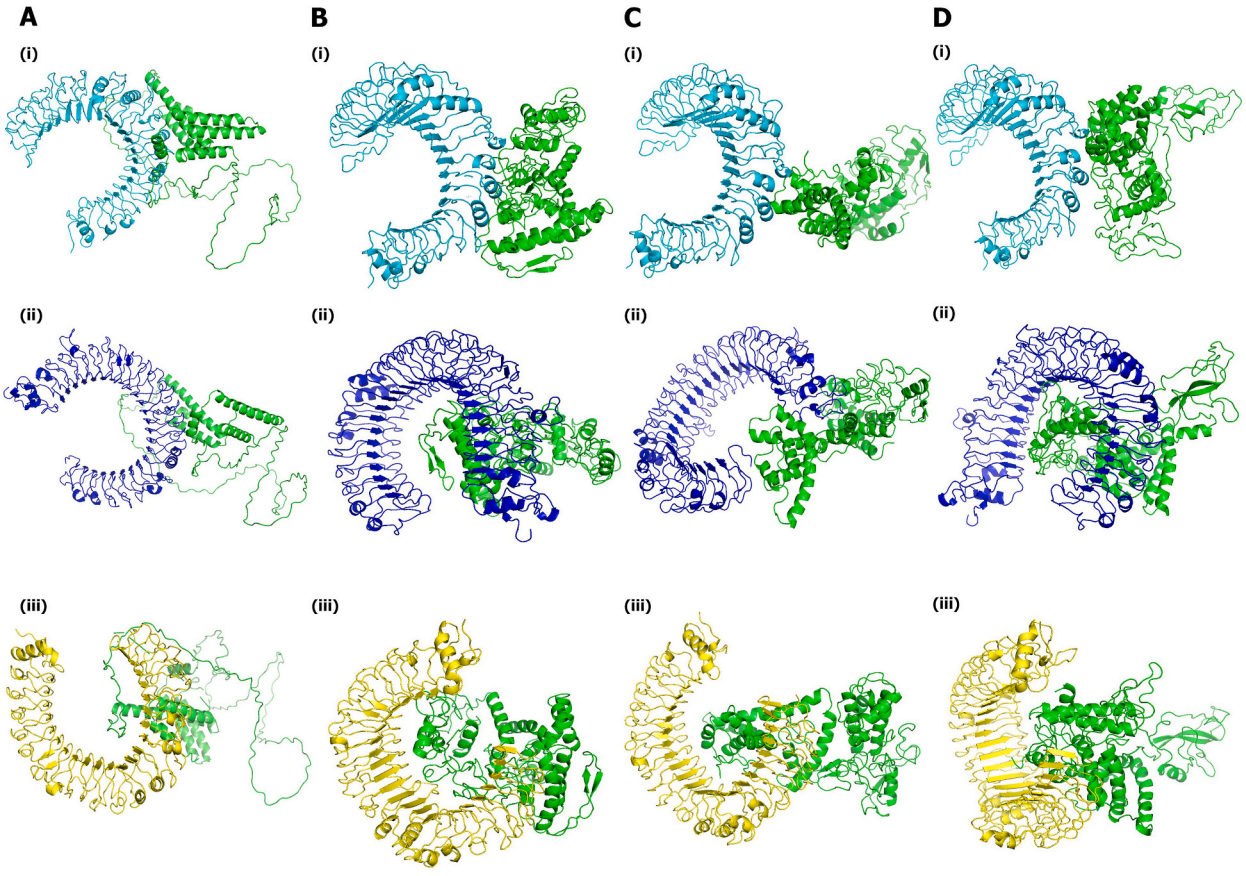

Fig. 6. Orientation and binding of vaccine constructs with TLR-2, TLR-3, and TLR4s. The constructs 1a, 1k, 1l and 1 m represented in A, B, C, and D panels respectively.

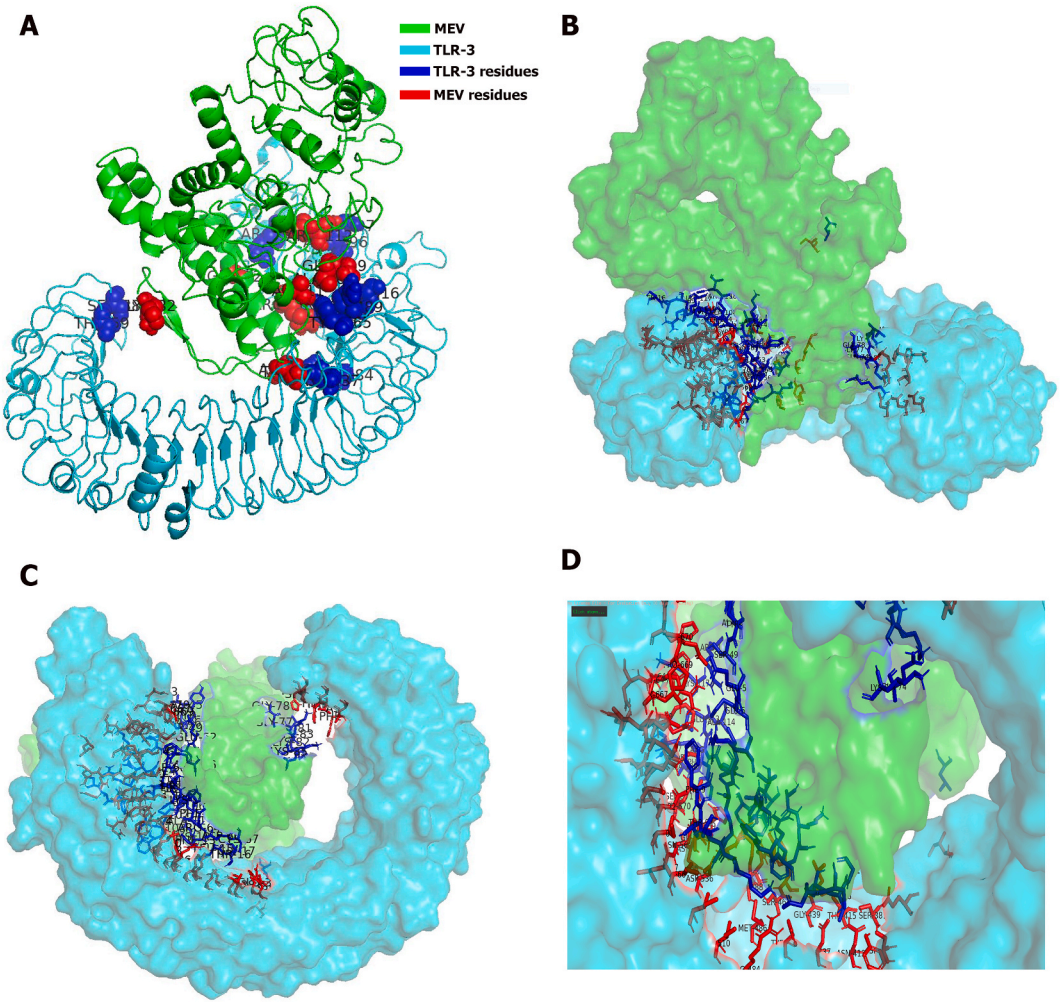

Fig. 7. TLR-3 binding interphase for MEV (1k) construct. A). 3D binding conformation for TLR-3 and MEV. The spheres shown indicate the interphase residues. B, C and D.

and TLR-4.

3.5. Immune response dynamic model generation for vaccine candidate

The multi-epitope vaccine interacts with various components of the immune system, including Toll-like receptors (TLRs), major histocompatibility complex class I and II (MHC-I and MHC-II), and B cell receptors (BCRs) [47]. TLRs are crucial in recognizing pathogen-associated molecular patterns of *Leishmania*, MHC molecules present antigens to T cells, and BCRs are responsible for B cell recognition of antigens [48]. Understanding the interactions between the vaccine and these immune molecules can provide insights into the recognition and activation processes involved in immune responses, and how the vaccine may induce or enhance these responses. The molecular dynamics simulation allows us to understand the interactions between the vaccine and various immune-related molecules, which can help assess the vaccine's stability, binding affinity, and potential efficacy. A multicomponent system with MEV (for clarity purposes 1k here onwards denoted by MEV), TLR-2, TLR-3, TLR-4, BCR and MHC-I and II was generated, energy minimized, equilibrated and simulated for 100 ns as described in methodology. The overall assembly of components was shown in (Fig. S2). The resulting trajectory was analysed for RMSD, RMSF, distance and dihedral angles.

The solvated average ensemble was used as reference and the RMSD of every component in the system in relation to initial structures were calculated. The solvated structure with final and starting structure was shown in (Fig. 9A). The arrangement of the components and the residues that are extended toward MEV were shown in (Fig. 9B and C). The RMSD through the simulation was calculated for all the components of the system and the results show, MEV, BCR has high RMSD deviation whereas MHC-II has minor deviation (Fig. 9D). Interestingly the BCR did not converge through the simulation and high deviation was observed. On the other hand the MEV converged and maintained stability without any major fluctuation through the simulation (Fig. 9D). Other components of the system showed minor fluctuation in RMSD though converged. The significant fluctuation in RMSD values observed for the vaccine and

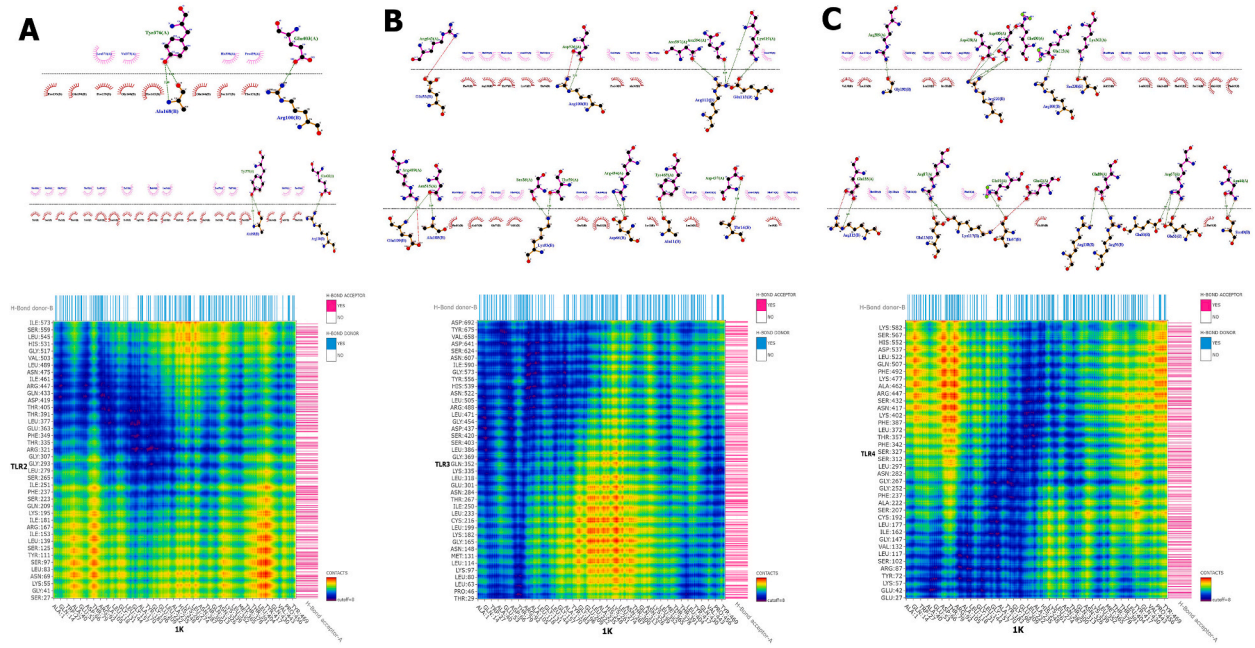

Fig. 8. Mapping the interactions of TLRs with MEV (1k) construct. A) top panelinteractions between TLR2- MEV, bottom panel-distance map constructed from Mapiya

Table 2
Construct 1k interactions with TLRs.

1K MEV	TLR2	IK MEV	TLR3	IK MEV	TLR4
Ala 168	Tyr 376	Arg 643	Glu 53	Gly 192	Arg 289
Arg 100	Glu 403	Asp 536	Arg 100	Arg 220	Asp 428, Asp 405, Gln 430
		Asn 597	Arg 112	Arg 100	Gln 115
		Asn 596	Arg 112	Ser 230	Lys 362
		Lys 619	Arg 112, Glu 113	Arg 112	Glu 135
		Arg 489	Glu 109	Glu 113	Arg 87
		Asn 515	Glu 109, Ala 108	Lys 117	Arg 87
		Ser 38	Lys 83	Lys 117	Glu 42
		Thr 59	Lys 83	Thr 97	Gln 91
		Arg 484	Asp 66	Arg 138	Glu 89
		Tyr 465	Ala 11	Arg 56	Glu 89
		Asp 437	Thr 16	Glu 53	Arg 67
				Glu 52	Arg 67
				Ser 49	Asn 44

BCR suggests that these molecules are undergoing substantial conformational changes throughout the simulation. Fluctuations in RMSD indicate structural flexibility, suggesting that the MEV and BCR may adopt different conformations or undergo rearrangements to accommodate binding interactions or dynamic changes in the simulation system. The varying fluctuation in RMSD values for MHC-II indicates relatively stable conformational behaviour during the simulation. MHC-II molecules are known to undergo conformational changes during antigen presentation, and the simulation trajectory suggests that MHC-II retains a relatively stable structure but has minor deviations from the initial conformation. As compared to other receptors, the RMSD values for TLR-2, TLR-3, and TLR-4 are not fluctuating and suggests that these molecules maintain a stable conformation during the simulation with minor conformational changes (Fig. 9D). These Toll-like receptors stability throughout the simulation suggests that their overall structure remains relatively unchanged and that their binding interfaces or ligand recognition sites undergo significant rearrangements during the simulated timeframe. To further assess the vicinity of MEV throughout simulation, RMSF was calculated. The residue fluctuation during simulation suggests that the residues 1–4, 7,8, 11, 125–210 of MEV showing above 15 Å fluctuation, whereas highest fluctuation was seen in TLR-3 spanning 1–5, 138–140, 159–161, 185–187, 666–670 residues (Fig. 9E). BCR has largest stretch of amino acids showing strong fluctuation for 1–113, 140–153, 179–211 and 217–257. For MHC-I and MHC-II also several residue stretches were showing strong fluctuation. Large spikes in RMSF can point to regions undergoing dynamic rearrangements, such as unfolding, domain movements, or transitions between different functional states. Though it is difficult to confirm from 100ns simulation, TLR-3 could be navigating towards MEV as inferred from RMSF values for specific stretches.

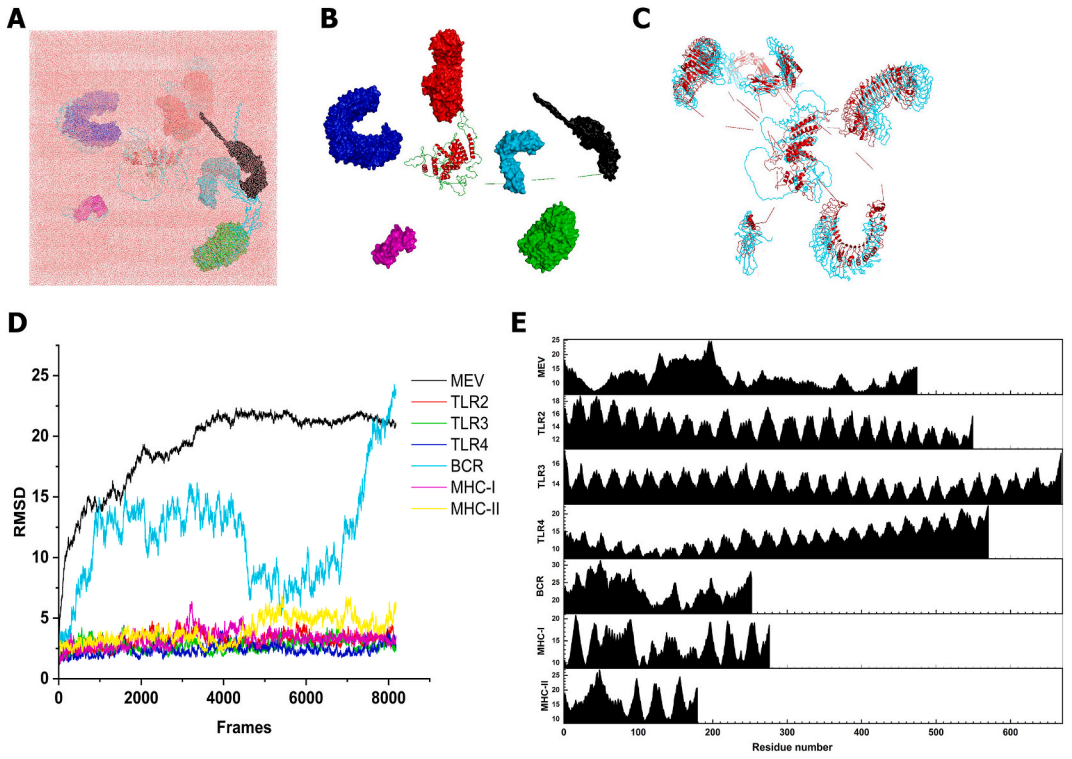

Fig. 9. Multicomponent assembly construction and validation for MEV construct. A) a solvated multicomponent system consisting 1k, TLR-2, TLR-3, TLR-4, BCR, MHC-I and.

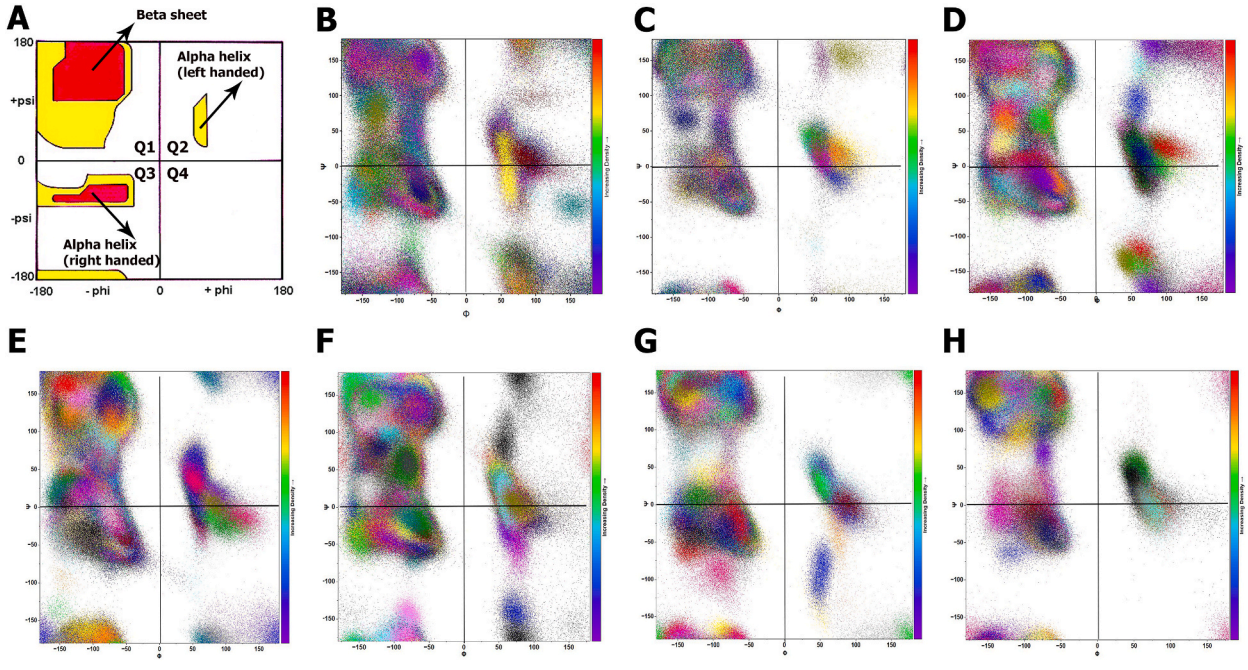

Fig. 10. Dihedral angle fluctuation analysis. A). typical plot for Ramachandran dihedrals. MEV, TLR-2, TLR-3, TLR-4, BCR, MHC-I and MHC-II quadrant analysis.

In addition, the dihedral angles of all the residues were calculated to explore the changes in individual residues dihedral over the time. The dihedral angles are important for understanding the conformational changes and flexibility of a molecule and also closely related to the potential energy landscape of a molecule. They provide the instantaneous positions of these angles during the simulation. The dihedral angles over the simulation was calculated from MD trajectory and a Ramachandran plot generated with Q1, Q2, Q3 and Q4 quadrants (Fig. 10A). Each dot in the plots indicate residue that has changes in dihedral angles over the 8178 frames of the trajectory each frame corresponding to 12.22 ps. The MEV dihedral distribution indicates most of the residues are fluctuating with spreading of the residues from Q1 to Q3, and Q2 to Q4 (Fig. 10B). The results could be an indication of flexibility and conformational changes of the MEV. It was expected as the molecules placed at center and may experience force from the surrounding molecules. Similar kind of distribution was observed in TLR-4 (Fig. 10F) suggests the TLR-4 is also has undergone conformational changes during simulation. Molecules BCR, MHC-I and MHC-II (Fig. 10C, G, 10H) have shown less spread though the dihedral angle fluctuation is present. Overall, the large variations in dihedral values indicate a more flexible molecule, while smaller variations suggest a more constrained or rigid structure.

3.6. MEV projected to move towards TLR-2, TLR-3 and MHC-II

The primary objective of conducting Molecular Dynamics (MD) simulations with immune components was to investigate their interactions with the Multiepitope Vaccine (MEV). This analysis aimed to discern whether, in the presence of numerous potential binding partners within the vicinity of MEV, these immune components exhibited any preferential binding behavior towards specific receptors. The distances between the immune components, namely TLR-4, MHC-I, and BCR, and the MEV were meticulously assessed and then normalized for uniform comparison.

The results of our analysis revealed interesting insights. Among the immune components, TLR-2, TLR-3, and MHC-II displayed distinct variations in their proximity to the MEV, as visually depicted in Fig. 11. Notably, TLR-3, a Toll-like receptor known for its role in recognizing double-stranded RNA, primarily associated with viral and parasitic infections, exhibited a noteworthy shift towards the MEV. This observed closeness of TLR-2 and TLR-3 to the MEV suggests the possibility of shared epitopes or motifs between the vaccine and parasitic components. This, in turn, raises intriguing implications regarding the potential activation of TLR-3 recognition, thus stimulating immune responses, as illustrated in Fig. 11. This interaction implies that the vaccine may be strategically designed to mimic parasitic elements, possibly aimed at eliciting a specific immune response against viral pathogens [49].

The closer distance between MHC-II and the MEV implies that the vaccine may possess epitopes that can bind to and be presented by MHC-II molecules (Fig. 11). This suggests that the vaccine is designed to elicit a helper T cell response, leading to the activation of adaptive immune responses. The interaction between TLR-3, MHC-II, and the MEV suggests that the vaccine has the potential to induce immune responses by engaging with these immune system components. The recognition of the vaccine by TLR-3 and the presentation of its epitopes by MHC-II molecules imply that the vaccine may have immunogenic properties, capable of triggering the activation of both innate and adaptive immune responses [50]. The proximity of TLR-3 and MHC-II to the MEV might indicate a favourable binding and recognition pattern, suggesting that the vaccine is designed to optimize the interaction with these immune system components. Such enhanced binding and recognition can contribute to the effectiveness of the vaccine by promoting robust immune responses, potentially leading to improved vaccine efficacy and protection against the targeted pathogens.

These results contribute valuable insights into the potential mechanisms of action and immune responses triggered by the multiepitope vaccine, shedding light on its ability to mimic parasitic components and engage with key immune receptors. Further research is necessary to fully comprehend the intricate dynamics underlying these interactions and their significance in vaccine design.

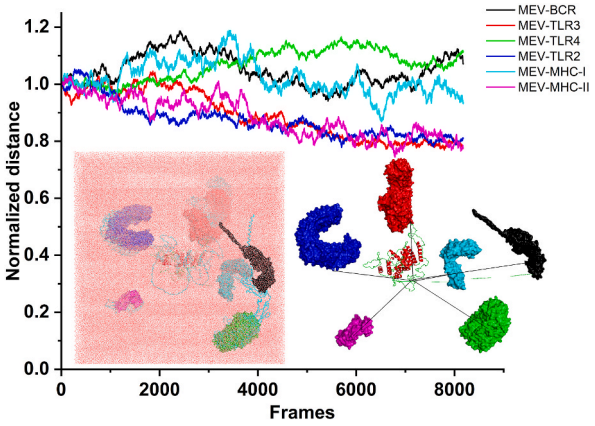

Fig. 11. Analysis of movement of immune components towards MEV (1k) during simulation. The normalized distance values indicate the TLR-2, TLR-3 and MHC-II.

3.7. In-silico characterization for solubility, expression and cloning of designed vaccine construct

Initially the construct 1k is in-*silico* cloned as described in methodology section (Fig. S3). The studies suggests that 1k is a strong vaccine candidate. The construct 1k comprised of 474 amino acids with a molecular weight of approximately 51 kDa. The Theoretical pI was found to be 9.51, suggesting that the vaccine construct is basic in nature with 37 negatively charged residues and 57 positively charged residues. The instability index was computed to be 33.13, classifying the protein as stable. The aliphatic index was estimated as 78.40, indicating that the protein is thermally stable over a wide temperature range. The grand average of hydro-pathicity (GRAVY) of the protein was found to be −0.081, suggesting that the protein is water-insoluble (hydro-phillic) (Supplementary data 3). Protein solubility predicted by protein-sol tool was estimated to be 0.560. To evaluate whether the sequence could be expressed in *E.coli* expression system, the protein sequence submitted to webserver ccSOLomics. The prediction suggests the construct is not soluble in when expressed in *E.coli* system with a solubility of 6 % (Fig. 12A). Further, the contribution of individual amino acids towards solubility indicate only few stretches of amino acids favours the solubility whereas most of the amino acid stretches comes under non-soluble region (Fig. 12B). Besides, the residues which do not favour solubility is substituted with another residue and see if the solubility enhances. There are few residues which can be replaced with another residue to increase the solubility whereas other residues 420–425 stretch is rigid and even replacing with other amino acid could not increase the overall solubility of the protein (Fig. 12B and C). Overall the results indicate the construct is not soluble in *E.coli* system and an insect or mammalian cell based expression system could facilitate better production of the construct.

4. Discussion

The development of an effective vaccine against leishmaniasis has been a challenge due to the complex biology of the parasite and the diverse clinical manifestations of the disease [51]. One of the obstacles is the immune evasion through phagolysosome enclosed parasite. Several researchers have attempted to design a suitable multiepitope vaccine exploiting epitopes selected from the parasite alone, which only favors the elimination of non-internalized parasites. Earlier studies suggested several key proteins expressing exclusively on host cells infected with *Leishmania* [12]. Targeting the infected host cells with internalized parasite could be beneficial in eliminating the parasite from system. These observations triggered to formulate an approach that targets both free parasite and internalized parasite harboring host cells.

The *Leishmania* parasite proteome was obtained from the Uniprot database (https://uniprot.org/) which consist of ~50000 proteins. The proteins that are not well explored or hypothetical in nature were excluded from the study. NetMHC4.0 and NetMHCII, BepiPred servers were used to predict the CTL, HTL and B-cell continuous epitopes. Over 27 proteins from infected host cells were found to be expressing upon infection and out of these only two proteins with long stretches were found to be strongly interacting with the MHC-I, MHC-II and BCR. Antigen processing and presentation is carried out by APCs, through MHC-I and MHC-II and BCRs. Dendritic cells along with macrophages have specialized roles in capturing, processing, and presenting antigens to T cells. The processed peptides or antigenic epitopes were recognized by Langerhans cells, and then migrate to draining lymph nodes to present processed antigens to T cells [52]. This initiates the adaptive immune response by presenting small peptides through major histocompatibility complex (MHC) class I or class II molecules. MHC class I molecules enable cytotoxic $CD8^+$ T cells to recognize endogenous peptides, while MHC class II molecules facilitate the presentation of exogenous peptides to $CD4^+$ T helper cells. The fragmentation of antigens is crucial for proper antigen presentation, as MHC class II molecules can only present peptides of a specific length [53]. A total of 13 proteins with potential epitopes for APC receptors were used for vaccine design. The conventional arrangement of epitopes such as BCE, HTL and CTL was found to be not immunogenic as determined by the VaxiJen2.0. Hence various combinations with a randomized arrangement were used to produce 13 vaccine constructs. Out of these constructs only three constructs passed the threshold (>0.5) for antigenicity. The 3D structure of the designed vaccine candidates suggests, they have high random coil content except 1a, 1k, 1l, and 1 m. The four structures have proper conformation and could be stable.

The immune response simulation for the constructs indicates most of them require only single dose to mount full scale immune response. All of the constructs assessed for their immune response inducing capacity. Upon injection of single dose of construct consisting 1000 molecules, the immunoglobulin (IgM, IgG, and IgM) levels were elevated specially to constructs 1a, 1l whereas only IgM levels are spiked in constructs 1k, 1 m. The overall response lasted for 100–150 days for some of the constructs. The immunoglobulin IgG and IgM levels are used to measure protection against specific antigen molecules [54]. They provide protection against the pathogen from which the epitopes were used in designing the vaccine candidate by neutralizing the pathogen [55]. A high proliferation of both helper and cytotoxic T-cells was observed throughout the simulation. The macrophages population is also consistently high through the simulation. Macrophages are the major effector cells responsible for destruction of the parasites [56]. Thus, appropriate activation of macrophages is crucial for eliminating this intracellular pathogen. Macrophage activation is generally divided into two functionally distinct types: classical and alternative activation. In classical activation, upon recognition of antigens on major histocompatibility complex (MHC) II, the differentiation of $CD4^+$ T cells into T helper type (Th) 1 primarily leads to the development of an inflammatory response. This response is characterized by the secretion of pro-inflammatory cytokines such as TNF-α, IL-1β, IL-6, IL-12, IL-18, and IL-23 [57]. The IFN-γ produced by Th1, stimulates macrophages to produce inducible nitric oxide synthase (iNOS, also known as NOS2), an enzyme which catalyzes *L-arginine* to generate nitric oxide (NO). NO is a toxic molecule that plays a major role in killing intracellular parasites [58]. The simulated immune response against MEV showed that the cytokines IFN-γ, TGF-β, IL-10 and IL-12 levels were high and lasted for several days. Therefore, the MEV induces both humoral and cellular immune response. The interaction of MEV with pathogen associated molecular patterns (PAMPs) like TLRs is essential for recognition and immune response [48]. The molecular docking between MEV and TLRs show strong interactions mediated by hydrogen bonds and

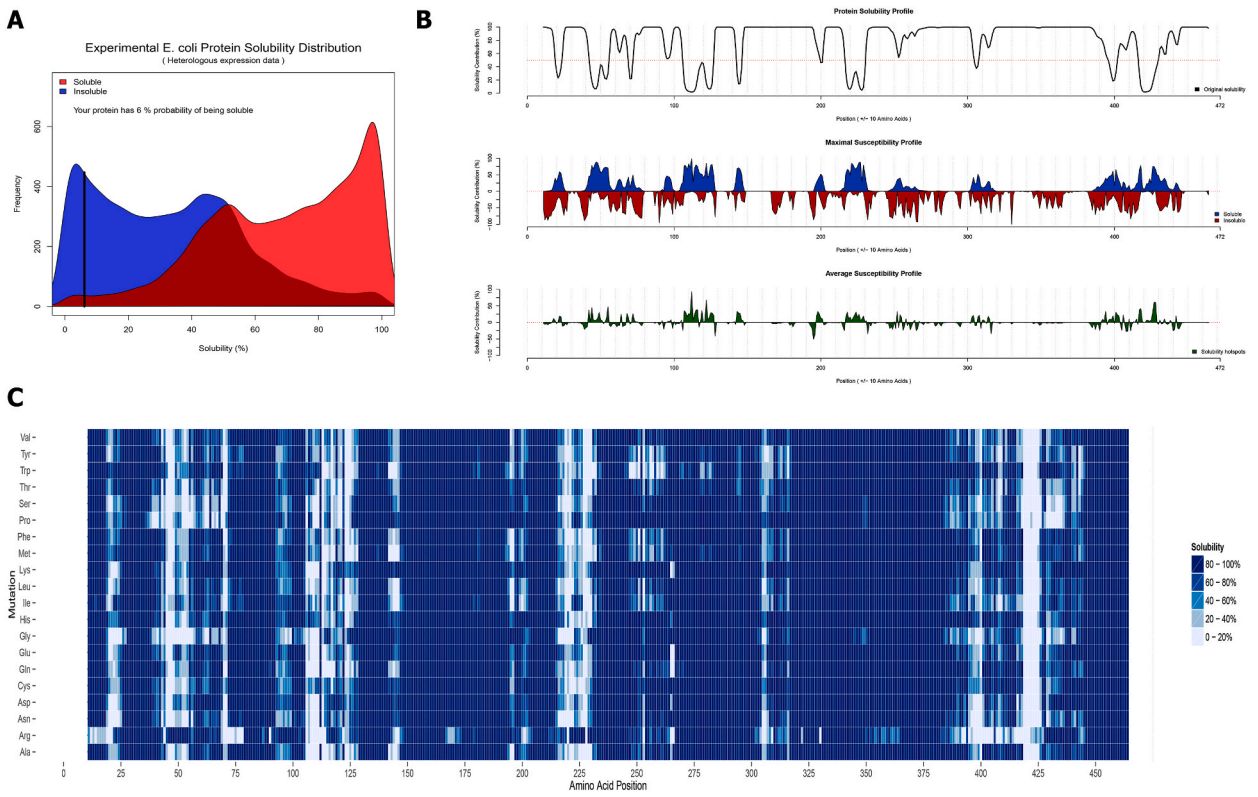

Fig. 12. Vaccine constructs soluble expression analysis. A). The sequence compared with existing soluble proteins database and plotted as percentage of.

hydrophobic interactions. More importantly the MEV showing strong affinity towards TLR-2, TLR-3 and TLR-4. The TLR-2 and TLR-4 are extracellular in nature while the TLR-3 is an intracellular protein [59]. It has been revealed that initial interaction of *Leishmania* lipophosphoglycan with TLR-2 activates the macrophages and the effects can be negative and positive on host cells and provide way to Th2 differentiation [60]. Earlier studies have suggested that TLR-4 involved in controlling the parasite growth in macrophages. The TLR-4 double knockout mice challenged with *L. major* infections showed reduction in growth at initial 24 h, and found increased parasite burden at later. In addition, the research also showed that the lack of TLR-4 results in impaired immune response [61]. Further, a multicomponent system consisting of vaccine construct MEV (1k), TLR-2, TLR-3, TLR-4, BCR, MHC-I and MHC-II was successfully generated and simulated for a 100 ns. The distance analysis indicate TLR-2, TLR-3 and MHC-II are moved towards MEV. The movement of MHC-II could be a positive indication that the vaccine effectively recognizes MHC-II and invoke immune response. A subtle movement of MHC-I also observed during simulation. The DCs can perform cross-presentation, which involves mobilizing MHC class I molecules to present exogenously derived antigens [62]. Moreover, the recognition of parasite components by the host cells (macrophages) is essential to dispose the infection [63]. The strong interaction of designed multi-epitope vaccine with TLR-2, TLR-4 indicate the MEV has potential to induce proper immune response. In summary, the designed vaccine candidate has great potential to be a vaccine candidate against *Leishmania* but further research need to be done to verify the findings.

CRediT authorship contribution statement

Sooram Banesh: Writing – original draft, Visualization, Validation, Methodology, Investigation, Formal analysis, Data curation, Conceptualization. **Neharika Gupta:** Methodology, Formal analysis. **Chethireddy Vihadhar Reddy:** Methodology, Investigation, Formal analysis. **Uppuladinne Mallikarjunachari:** Resources, Methodology, Data curation. **Nupoor Patil:** Methodology, Formal analysis, Data curation. **Sonavane Uddhavesh:** Resources, Methodology, Data curation. **Prakash Saudagar:** Writing – review & editing, Validation, Supervision, Software, Resources, Project administration, Methodology, Formal analysis, Data curation, Conceptualization.

Declaration of competing interest

The authors declare that they have no known competing financial interests or personal relationships that could have appeared to influence the work reported in this paper.

Acknowledgements

Sooram Banesh (SB) thanks NIT Warangal for fellowship support. The authors thank Arnav Bhukhmaria (research intern) for helping in analysis. Authors acknowledge the Bioinformatics Resources and Applications Facility (BRAF), of C-DAC, Pune, for providing a supercomputing facility to carryout molecular dynamics simulations.

Appendix A. Supplementary data

Supplementary data to this article can be found online at https://doi.org/10.1016/j.heliyon.2024.e31306.

References

[1] A. Martiny, J. Saad-Nehme, J.R. Meyer-Fernandes, W. de Souza, M.A. Vannier-Santos, RT1–INVASION AND INTRACELLULAR BEHAVIOR IN PROTOZOA RT1-ALTERATION OF MACROPHAGE CELLULAR SIGNALING CASCADES BY LEISHMANIA PARASITES.
[2] M. Akhoundi, K. Kuhls, A. Cannet, J. Votýpka, P. Marty, P. Delaunay, D. Sereno, A historical overview of the classification, evolution, and dispersion of Leishmania parasites and sandflies, PLoS Neglected Trop. Dis. 10 (3) (2016) e0004349.
[3] J.A. Ruiz-Postigo, S. Jain, A. Mikhailov, A.N. Maia-Elkhoury, S. Valadas, S. Warusavithana, M. Osman, Z. Lin, A. Beshah, A. Yajima, Global leishmaniasis surveillance: 2019-2020, a baseline for the 2030 roadmap/Surveillance mondiale de la leishmaniose: 2019-2020, une periode de reference pour la feuille de route a l'horizon 2030, Wkly. Epidemiol. Rec. 96 (35) (2021) 401–420.
[4] R. Killick-Kendrick, The life-cycle of Leishmania in the sandfly with special reference to the form infective to the vertebrate host, Ann. Parasitol. Hum. Comp. 65 (1990) 37–42.
[5] R. Pulvertaft, G. Hoyle, Stages in the life-cycle of Leishmania donovani, Trans. R. Soc. Trop. Med. Hyg. 54 (2) (1960) 191–196.
[6] A.J. Davis, H.W. Murray, E. Handman, Drugs against leishmaniasis: a synergy of technology and partnerships, Trends Parasitol. 20 (2) (2004) 73–76.
[7] L.F. Oliveira, A.O. Schubach, M.M. Martins, S.L. Passos, R.V. Oliveira, M.C. Marzochi, C.A. Andrade, Systematic review of the adverse effects of cutaneous leishmaniasis treatment in the New World, Acta Trop. 118 (2) (2011) 87–96.
[8] M. Moafi, H. Rezvan, R. Sherkat, R. Taleban, Leishmania vaccines entered in clinical trials: a review of literature, Int. J. Prev. Med. 10 (2019).
[9] R. Velez, M. Gallego, Commercially approved vaccines for canine leishmaniosis: a review of available data on their safety and efficacy, Trop. Med. Int. Health 25 (5) (2020) 540–557.
[10] A.N. Oli, W.O. Obialor, M.O. Ifeanyichukwu, D.C. Odimegwu, J.N. Okoyeh, G.O. Emechebe, S.A. Adejumo, G.C. Ibeanu, Immunoinformatics and Vaccine Development: an Overview, ImmunoTargets and Therapy, 2020, pp. 13–30.
[11] M. Comanducci, S. Bambini, B. Brunelli, J. Adu-Bobie, B. Aricò, B. Capecchi, M.M. Giuliani, V. Masignani, L. Santini, S. Savino, NadA, a novel vaccine candidate of Neisseria meningitidis, The Journal of experimental medicine 195 (11) (2002) 1445–1454.
[12] J.P.B.d. Menezes, T.F.d. Almeida, A.L.d.O.A. Petersen, C.E.S. Guedes, M. Mota, J.G.B. Lima, L.C. Palma, G.A. Buck, M.A. Krieger, C.M. Probst, Proteomic analysis reveals differentially expressed proteins in macrophages infected with Leishmania amazonensis or Leishmania major, Microb. Infect. 15 (8–9) (2013) 579–591.
[13] D. Nandan, E. Chen, F. Chang, K.-M. Moon, L.J. Foster, N. Reiner, Comprehensive proteomic analysis of autophagosomes derived from Leishmania-infected macrophages, PLoS One 18 (4) (2023) e0284026.
[14] V. Thumuluri, J.J. Almagro Armenteros, A.R. Johansen, H. Nielsen, O. Winther, DeepLoc 2.0: multi-label subcellular localization prediction using protein language models, Nucleic acids research 50 (W1) (2022) W228–W234.
[15] J. Hallgren, K.D. Tsirigos, M.D. Pedersen, J.J. Almagro Armenteros, P. Marcatili, H. Nielsen, A. Krogh, O. Winther, DeepTMHMM predicts alpha and beta transmembrane proteins using deep neural networks, bioRxiv (2022), 2022.04. 08.487609.
[16] M. Nielsen, C. Lundegaard, P. Worning, S.L. Lauemøller, K. Lamberth, S. Buus, S. Brunak, O. Lund, Reliable prediction of T-cell epitopes using neural networks with novel sequence representations, Protein Sci. 12 (5) (2003) 1007–1017.
[17] J. Greenbaum, The Immune Epitope Database and Analysis Resource (IEDB), EMBRACE Bioinformatics of Immunology Workshop, La Jolla Institute for Allergy and Immunology, Citeseer, Lyngby, Denmark, 2007.
[18] B. Reynisson, B. Alvarez, S. Paul, B. Peters, M. Nielsen, NetMHCpan-4.1 and NetMHCIIpan-4.0: improved predictions of MHC antigen presentation by concurrent motif deconvolution and integration of MS MHC eluted ligand data, Nucleic acids research 48 (W1) (2020) W449–W454.
[19] J.N. Clifford, M.H. Høie, S. Deleuran, B. Peters, M. Nielsen, P. Marcatili, BepiPred-3.0: improved B-cell epitope prediction using protein language models, Protein Sci. 31 (12) (2022) e4497.
[20] M. Chawla-Sarkar, D.J. Lindner, Y.-F. Liu, B. Williams, G.C. Sen, R.H. Silverman, E.C. Borden, Apoptosis and interferons: role of interferon-stimulated genes as mediators of apoptosis, Apoptosis 8 (2003) 237–249.
[21] P. Li, Q. Du, Z. Cao, Z. Guo, J. Evankovich, W. Yan, Y. Chang, L. Shao, D.B. Stolz, A. Tsung, Interferon-gamma induces autophagy with growth inhibition and cell death in human hepatocellular carcinoma (HCC) cells through interferon-regulatory factor-1 (IRF-1), Cancer letters 314 (2) (2012) 213–222.
[22] S.K. Dhanda, P. Vir, G.P. Raghava, Designing of interferon-gamma inducing MHC class-II binders, Biol. Direct 8 (1) (2013) 1–15.
[23] G. Mackaness, Cellular Immunity and the Parasite, Immunity to Blood Parasites of Animals and Man, 1977, pp. 65–73.
[24] M. Li, Y. Jiang, T. Gong, Z. Zhang, X. Sun, Intranasal vaccination against HIV-1 with adenoviral vector-based nanocomplex using synthetic TLR-4 agonist peptide as adjuvant, Mol. Pharm. 13 (3) (2016) 885–894.
[25] A.U. Danazumi, S.I. Gital, S. Idris, L.B. Dibba, E.O. Balogun, M.W. Górna, Immunoinformatic design of a putative multi-epitope vaccine candidate against Trypanosoma brucei gambiense, Comput. Struct. Biotechnol. J. 20 (2022) 5574–5585.
[26] I. Dimitrov, D.R. Flower, I. Doytchinova, AllerTOP-a server for in silico prediction of allergens, BMC bioinformatics, BioMed Central (2013) 1–9.
[27] P. Blast, Search Protein Databases Using a Protein Query, 2017. Blast. ncbi. nlm. nih. gov (2017).
[28] S. Gupta, P. Kapoor, K. Chaudhary, A. Gautam, R. Kumar, O.S.D.D. Consortium, G.P. Raghava, In silico approach for predicting toxicity of peptides and proteins, PLoS One 8 (9) (2013) e73957.
[29] R.A. Laskowski, M.W. MacArthur, D.S. Moss, J.M. Thornton, PROCHECK: a program to check the stereochemical quality of protein structures, J. Appl. Crystallogr. 26 (2) (1993) 283–291.
[30] M. Wiederstein, M.J. Sippl, ProSA-web: interactive web service for the recognition of errors in three-dimensional structures of proteins, Nucleic acids research 35 (suppl_2) (2007) W407–W410.
[31] N. Rapin, O. Lund, F. Castiglione, Immune system simulation online, Bioinformatics 27 (14) (2011) 2013–2014.
[32] J. Jumper, R. Evans, A. Pritzel, T. Green, M. Figurnov, O. Ronneberger, K. Tunyasuvunakool, R. Bates, A. Žídek, A. Potapenko, Highly accurate protein structure prediction with AlphaFold, Nature 596 (7873) (2021) 583–589.
[33] D. Kozakov, D.R. Hall, B. Xia, K.A. Porter, D. Padhorny, C. Yueh, D. Beglov, S. Vajda, The ClusPro web server for protein–protein docking, Nat. Protoc. 12 (2) (2017) 255–278.
[34] A.C. Wallace, R.A. Laskowski, J.M. Thornton, LIGPLOT: a program to generate schematic diagrams of protein-ligand interactions, Protein Eng. Des. Sel. 8 (2) (1995) 127–134.

[35] R. Salomon-Ferrer, D.A. Case, R.C. Walker, An overview of the Amber biomolecular simulation package, Wiley Interdiscip. Rev. Comput. Mol. Sci. 3 (2) (2013) 198–210.
[36] D.A. Case, K. Belfon, I. Ben-Shalom, S.R. Brozell, D.S. Cerutti, T.E. Cheatham, V. Cruzeiro, T. Darden, R. Duke, G. Giambasu, Amber 2020, University of california, San Francisco, 2020.
[37] S. Jo, T. Kim, V.G. Iyer, W. Im, CHARMM-GUI: a web-based graphical user interface for CHARMM, J. Comput. Chem. 29 (11) (2008) 1859–1865.
[38] A. Grote, K. Hiller, M. Scheer, R. Münch, B. Nörtemann, D.C. Hempel, D. Jahn, JCat: a novel tool to adapt codon usage of a target gene to its potential expression host, Nucleic acids research 33 (suppl_2) (2005) W526–W531.
[39] S.G. Reed, M.T. Orr, C.B. Fox, Key roles of adjuvants in modern vaccines, Nature medicine 19 (12) (2013) 1597–1608.
[40] F. Mancini, O. Rossi, F. Necchi, F. Micoli, OMV vaccines and the role of TLR agonists in immune response, Int. J. Mol. Sci. 21 (12) (2020) 4416.
[41] M. Negahdaripour, N. Nezafat, M. Eslami, M.B. Ghoshoon, E. Shoolian, S. Najafipour, M.H. Morowvat, A. Dehshahri, N. Erfani, Y. Ghasemi, Structural vaccinology considerations for in silico designing of a multi-epitope vaccine, Infect. Genet. Evol. 58 (2018) 96–109.
[42] N. Alharbi, M. Skwarczynski, I. Toth, The influence of component structural arrangement on peptide vaccine immunogenicity, Biotechnol. Adv. (2022) 108029.
[43] R. Racine, G.M. Winslow, IgM in microbial infections: taken for granted? Immunol. Lett. 125 (2) (2009) 79–85.
[44] A. Neurath, S. Kent, N. Strick, K. Parker, Identification and chemical synthesis of a host cell receptor binding site on hepatitis B virus, Cell 46 (3) (1986) 429–436.
[45] F.F. Tuon, V.S. Amato, H.A. Bacha, T. AlMusawi, M.I. Duarte, V. Amato Neto, Toll-like receptors and leishmaniasis, Infect. Immun. 76 (3) (2008) 866–872.
[46] J.F. Flandin, F. Chano, A. Descoteaux, RNA interference reveals a role for TLR-2 and TLR-3 in the recognition of Leishmania donovani promastigotes by interferon–γ-primed macrophages, Eur. J. Immunol. 36 (2) (2006) 411–420.
[47] P. Pan, F. Zhu, S. Ma, M. Rao, P. Zhang, W. Peng, Y. Cui, H. Yang, C. Tan, J. Chen, Immunoinformatics Approaches for Developing Multi-Epitope Subunit Vaccines to Combat Acinetobacter Baumannii, 2022.
[48] K. Dolasia, M.K. Bisht, G. Pradhan, A. Udgata, S. Mukhopadhyay, TLRs/NLRs: shaping the landscape of host immunity, Int. Rev. Immunol. 37 (1) (2018) 3–19.
[49] G.E. Kaiko, J.C. Horvat, K.W. Beagley, P.M. Hansbro, Immunological decision-making: how does the immune system decide to mount a helper T-cell response? Immunology 123 (3) (2008) 326–338.
[50] I. Fatima, S. Ahmad, S.W. Abbasi, U.A. Ashfaq, F. Shahid, M.T. ul Qamar, A. Rehman, K.S. Allemailem, Designing of a multi-epitopes-based peptide vaccine against rift valley fever virus and its validation through integrated computational approaches, Comput. Biol. Med. 141 (2022) 105151.
[51] S. Srivastava, P. Shankar, J. Mishra, S. Singh, Possibilities and challenges for developing a successful vaccine for leishmaniasis, Parasites Vectors 9 (2016) 1–15.
[52] H. Moll, H. Fuchs, C. Blank, M. Röllinghoff, Langerhans cells transport Leishmania major from the infected skin to the draining lymph node for presentation to antigen-specific T cells, Eur. J. Immunol. 23 (7) (1993) 1595–1601.
[53] K.L. Rock, E. Reits, J. Neefjes, Present yourself! By MHC class I and MHC class II molecules, Trends Immunol. 37 (11) (2016) 724–737.
[54] A. Ademokun, Y.C. Wu, V. Martin, R. Mitra, U. Sack, H. Baxendale, D. Kipling, D.K. Dunn-Walters, Vaccination-induced changes in human B-cell repertoire and pneumococcal IgM and IgA antibody at different ages, Aging Cell 10 (6) (2011) 922–930.
[55] A.V. Wisnewski, J.C. Luna, C.A. Redlich, Human IgG and IgA responses to COVID-19 mRNA vaccines, PLoS One 16 (6) (2021) e0249499.
[56] D. Liu, J.E. Uzonna, The early interaction of Leishmania with macrophages and dendritic cells and its influence on the host immune response, Front. Cell. Infect. Microbiol. 2 (2012) 83.
[57] C. dos Santos Meira, L. Gedamu, Protective or detrimental? understanding the role of host immunity in leishmaniasis, Microorganisms 7 (12) (2019) 695.
[58] F. Liew, Y. Li, S. Millott, Tumour necrosis factor (TNF-alpha) in leishmaniasis. II. TNF-alpha-induced macrophage leishmanicidal activity is mediated by nitric oxide from L-arginine, Immunology 71 (4) (1990) 556.
[59] M.S. Faria, F.C. Reis, A.P.C. Lima, Toll-like receptors in leishmania infections: guardians or promoters? Journal of parasitology research 2012 (2012).
[60] G. Kavoosi, S. Ardestani, A. Kariminia, The involvement of TLR-2 in cytokine and reactive oxygen species (ROS) production by PBMCs in response to Leishmania major phosphoglycans (PGs), Parasitology 136 (10) (2009) 1193–1199.
[61] P. Kropf, N. Freudenberg, C. Kalis, M. Modolell, S. Herath, C. Galanos, M. Freudenberg, I. Müller, Infection of C57BL/10ScCr and C57BL/10ScNCr mice with Leishmania major reveals a role for Toll-like receptor 4 in the control of parasite replication, J. Leukoc. Biol. 76 (1) (2004) 48–57.
[62] J.F. Fonteneau, D.G. Kavanagh, M. Lirvall, C. Sanders, T.L. Cover, N. Bhardwaj, M. Larsson, Characterization of the MHC class I cross-presentation pathway for cell-associated antigens by human dendritic cells, Blood 102 (13) (2003) 4448–4455.
[63] L. David Sibley, Invasion and intracellular survival by protozoan parasites, Immunol. Rev. 240 (1) (2011) 72–91.